iScience

CellPress
OPEN ACCESS

Article

Oral metformin transiently lowers post-prandial glucose response by reducing the apical expression of sodium-glucose co-transporter 1 in enterocytes

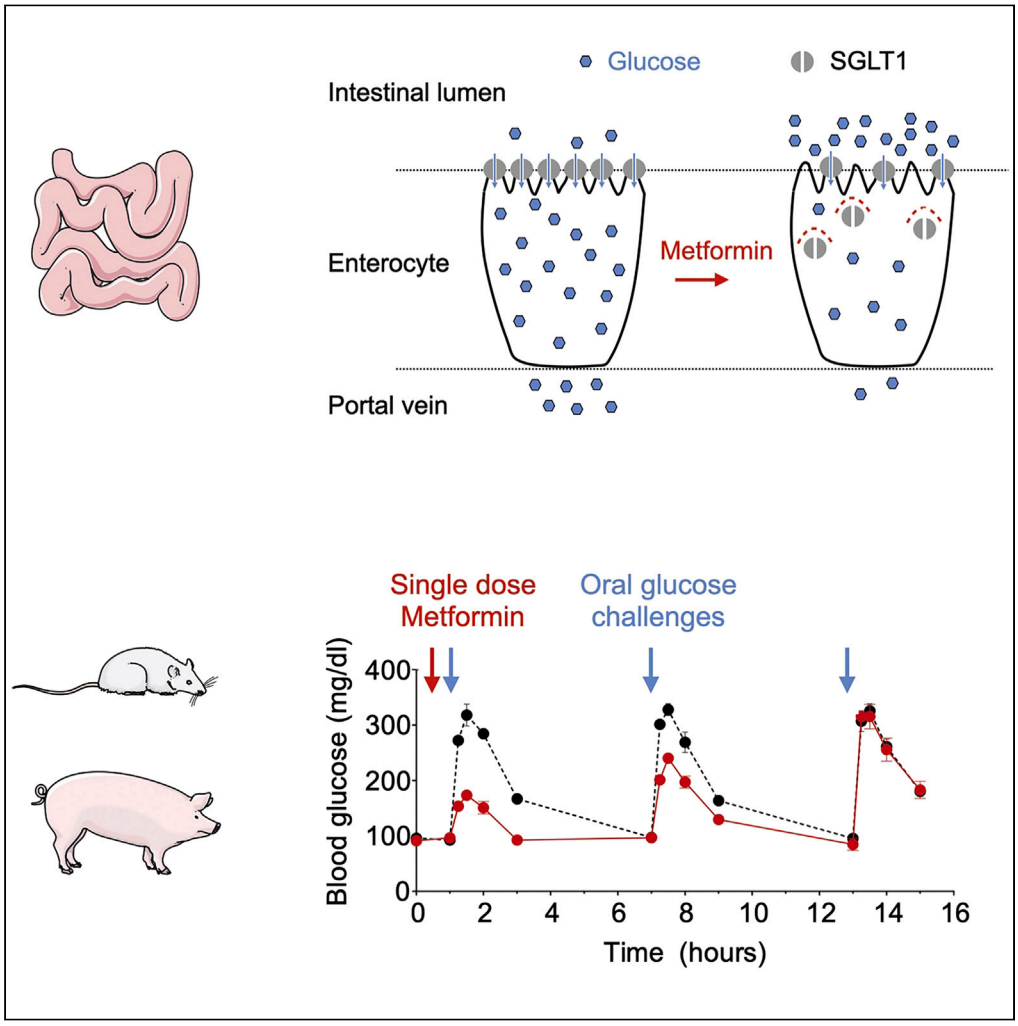

Lorea Zubiaga, Olivier Briand, Florent Auger, ..., Damien Huglo, Sophie Lestavel, François Pattou

francois.pattou@univ-lille.fr

Highlights

Metformin transiently reduces SGLT1 apical expression in enterocytes

Metformin acutely reduces SGLT1-mediated enterocyte glucose uptake

Oral metformin acutely reduces SGLT1-mediated post-prandial glucose response

Zubiaga et al., iScience 26, 106057
April 21, 2023 © 2023
https://doi.org/10.1016/j.isci.2023.106057

iScience

CellPress
OPEN ACCESS

Article

Oral metformin transiently lowers post-prandial glucose response by reducing the apical expression of sodium-glucose co-transporter 1 in enterocytes

Lorea Zubiaga,[1,10] Olivier Briand,[2,10] Florent Auger,[3,10] Veronique Touche,[2] Thomas Hubert,[1] Julien Thevenet,[1] Camille Marciniak,[1] Audrey Quenon,[1] Caroline Bonner,[1,4] Simon Peschard,[2,10] Violeta Raverdy,[1] Mehdi Daoudi,[1] Julie Kerr-Conte,[1] Gianni Pasquetti,[1] Hermann Koepsell,[5] Daniela Zdzieblo,[5] Markus Mühlemann,[5] Bernard Thorens,[6] Nathalie D. Delzenne,[7] Laure B. Bindels,[7] Benoit Deprez,[8] Marie C. Vantyghem,[1] Blandine Laferrère,[9] Bart Staels,[2] Damien Huglo,[3] Sophie Lestavel,[2] and François Pattou[1,11,*]

SUMMARY

Metformin (MET) is the most prescribed antidiabetic drug, but its mechanisms of action remain elusive. Recent data point to the gut as MET's primary target. Here, we explored the effect of MET on the gut glucose transport machinery. Using human enterocytes (Caco-2/TC7 cells) *in vitro*, we showed that MET transiently reduced the apical density of sodium-glucose transporter 1 (SGLT1) and decreased the absorption of glucose, without changes in the mRNA levels of the transporter. Administered 1 h before a glucose challenge in rats (Wistar, GK), C57BL6 mice and mice pigs, oral MET reduced the post-prandial glucose response (PGR). This effect was abrogated in SGLT1-KO mice. MET also reduced the luminal clearance of 2-(^{18}F)-fluoro-2-deoxy-D-glucose after oral administration in rats. In conclusion, oral metformin transiently lowers post-prandial glucose response by reducing the apical expression of SGLT1 in enterocytes, which may contribute to the clinical effects of the drug.

INTRODUCTION

Metformin (MET) is a widely used glucose-lowering agent in the clinic for type 2 diabetes (T2D) with beneficial effects on cardiovascular diseases and cancer.[1,2] MET decreases hepatic endogenous glucose production[3,4] and increases insulin sensitivity.[5–7] Alternatively, recent data suggest that the primary glucose-lowering effect of MET resides in the gut, not in the circulation.[8–11] Such mechanisms likely explain the decrease in the post-prandial glucose response (PGR) induced by oral MET treatment, independently of changes in fasting glucose.[12,13] The proposed gastrointestinal mechanisms of MET include gastric emptying,[14] intestinal uptake and utilization of blood glucose,[15–17] bile acid trafficking,[18–20] glucagon-like peptide-1 (GLP-1) secretion,[21] or changes in the gut microbiota.[22,23] An effect of MET in dietary glucose absorption has been also suggested in animals[24] and humans.[25] However, the effect of MET at the level of the enterocyte glucose transport machinery remains controversial. Lenzen et al.[26] described the increased intestinal expression of *Slc5a1*, the gene encoding sodium-glucose transporter 1 (SGLT1), in rats treated with MET twice daily for a period of three days. Sakar et al. reported a decrease in SGLT1 protein levels in the apical membrane with an increase in type 2 facilitated glucose transporter (GLUT2) expression, resulting in a net increase in glucose absorption via adenosine monophosphate kinase (AMPK) activation.[27] Conversely, Horakova et al. provided indirect evidence suggesting that MET modulates intestinal glucose transport in an AMPK-independent manner, but with increased passage of glucose from the lumen to the cell and decreased from the cell to the blood.[28] Overall, the effect of MET on intestinal glucose trafficking remains highly debated.[29] In the present study, we demonstrate that a single dose of MET reduces the apical density of SGLT1 in the enterocyte resulting in an acute and transient decrease in the intestinal absorption of intraluminal glucose and a reduction in the PGR.

[1]University of Lille, Centre Hospitalier Universitaire de Lille, European Genomic Institute for Diabetes, Inserm UMR-1190, 59000 Lille, France

[2]University of Lille, Inserm, Centre Hospitalier Universitaire de Lille, Institut Pasteur de Lille, U1011-EGID, 59000 Lille, France

[3]University of Lille, Preclinical Imaging Core Facility, 59000 Lille, France

[4]Institut Pasteur de Lille, 59000 Lille, France

[5]Institute of Anatomy and Cell Biology, University of Würzburg, 97070 Würzburg, Germany

[6]University of Lausanne, Center for Integrative Genomics, Lausanne, Switzerland

[7]Université catholique de Louvain, Metabolism and Nutrition Research Group, Louvain Drug Research Institute, Brussels, Belgium

[8]University of Lille, Centre Hospitalier Universitaire de Lille, European Genomic Institute for Diabetes, Inserm UMR-1177, 59000 Lille, France

[9]Department of Medicine, New York Nutrition Obesity Research Center, Columbia University College of Physicians and Surgeons, New York, NY, USA

[10]These authors contributed equally

[11]Lead contact

*Correspondence: francois.pattou@univ-lille.fr

https://doi.org/10.1016/j.isci.2023.106057

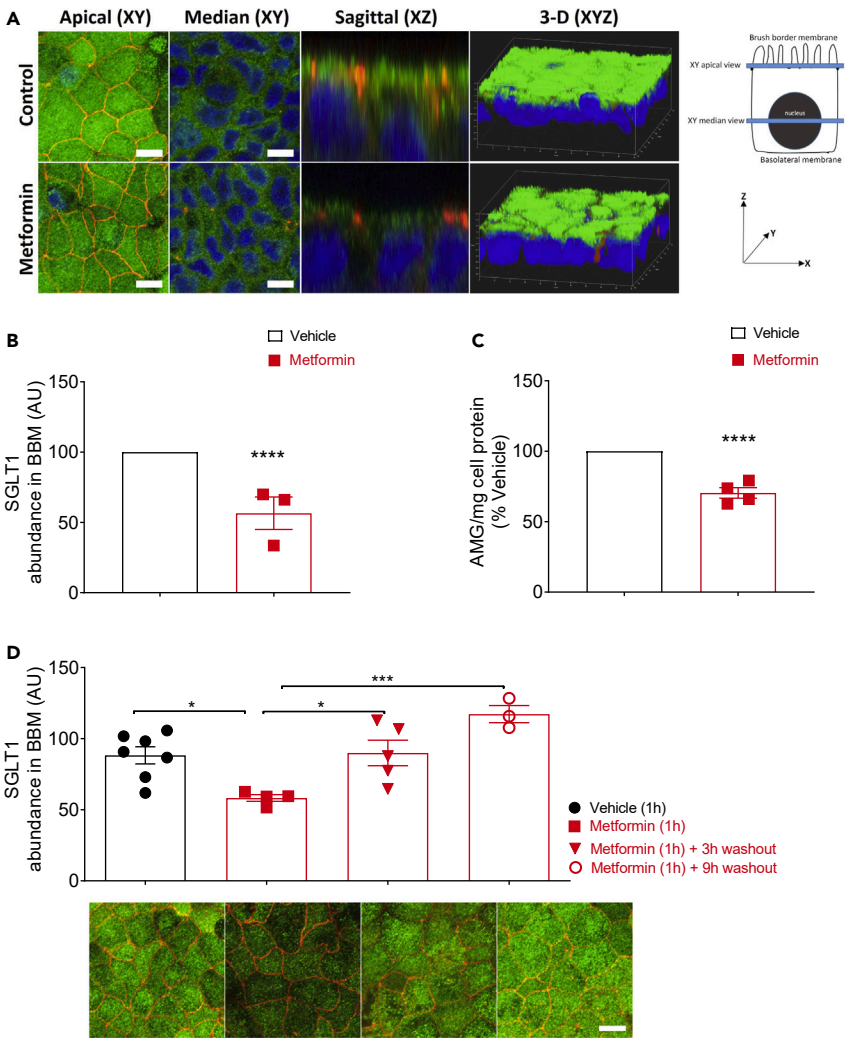

Figure 1. Effects of a single dose of 10 mM metformin (MET) in Caco-2/TC7 cells after 1 h

(A) Representative immunofluorescence images (n ≥ 12 in total) of SGLT1 in Caco-2/TC7 cells after a 1-h incubation with vehicle or MET. Scale bar, 10 μm. The schematic diagram illustrates the plane of the images relative to the morphology of the enterocytes.

(B) Quantification using arbitrary units (AU) of SGLT1 abundance in the brush border membrane (BBM) by fluoroscopy (each dot represents one experiment performed with 3 biological replicates).

(C) α-Methyl-D-(^{14}C)-glucopyranoside (AMG) apical uptake after 1 h of MET incubation (each dot represents one experiment performed with four biological replicates).

(D) Quantification of SGLT1 abundance in the BBM after a 1-h incubation with MET and two different washout times simulating the clearance of MET *in vivo* (3 and 9 h) and representative immunofluorescent images for each condition. Scale bar, 20 μm. Each dot represents one experiment performed with two biological replicates. Data are mean ± SEM *p < 0.05 ***p < 0.001 and ****p < 0.0001 by two-way ANOVA(B, C) or one-way ANOVA(D), MET vs. vehicle.

RESULTS

MET reduces the apical abundance of SGLT1 in a human intestinal Caco-2/TC7 cell model

First, we explored the direct effect of MET on SGLT1 biology in a human intestinal cell model. After a 1 h incubation of polarized Caco-2/TC7 cells with 10 mM MET, a dose that was chosen to approximate the concentration of metformin present at the apical side of the enterocytes 1 h after the ingestion of a single dose of metformin,[30] the apical presence of SGLT1 in the brush border membrane (BBM), was significantly lower compared to vehicle-treated cells (Figures 1A and 1B). This reduction in SGLT1 abundance was accompanied by a lower degree of apical uptake of α-methyl-D-[^{14}C]-glucopyranoside (AMG) (Figure 1C), a non-metabolizable glucose analog specifically transported by SGLT1.[31] Moreover, SGLT1 abundance in

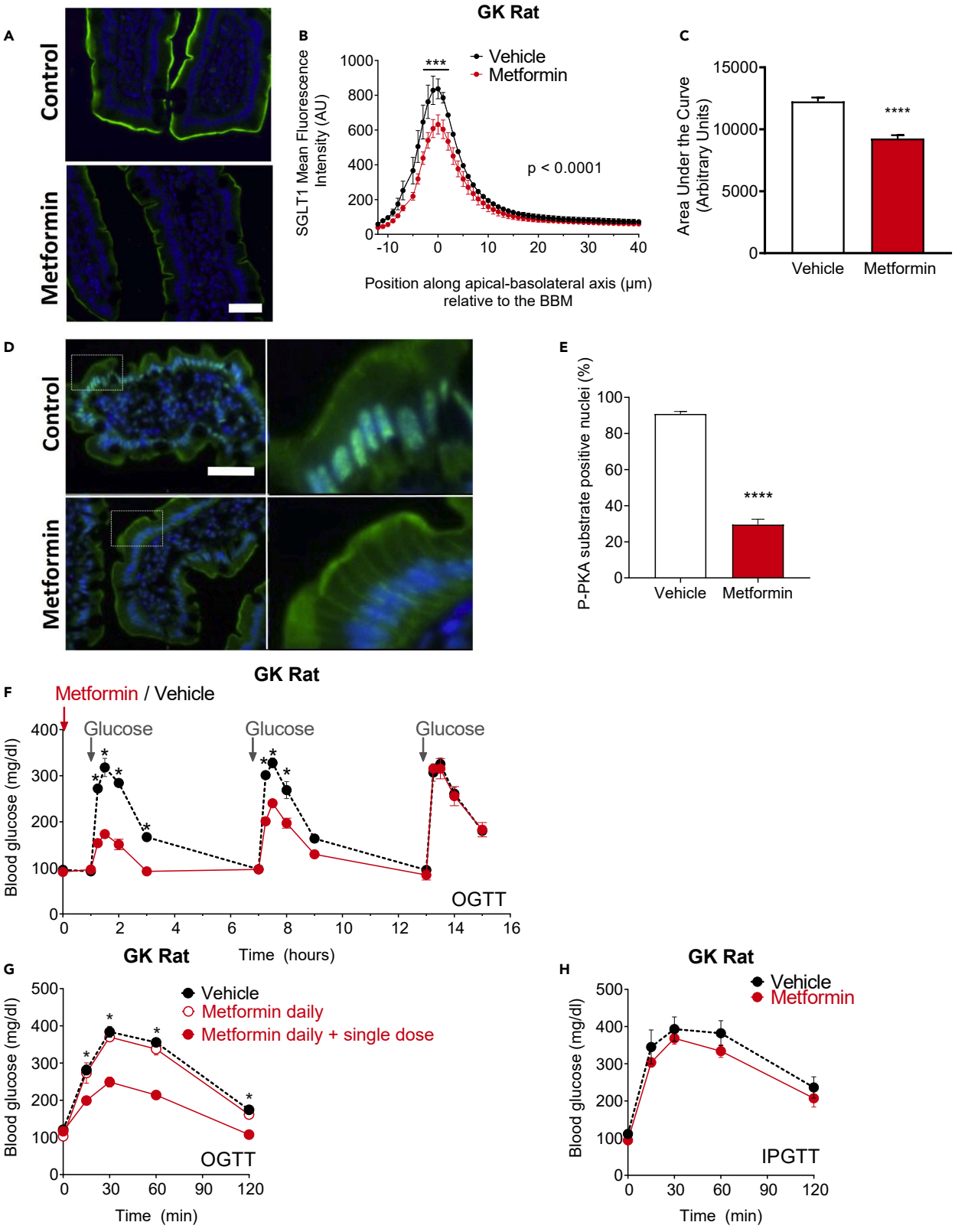
A
Control
Metformin
B
GK Rat
SGLT1 Mean Fluorescence Intensity (AU)
Vehicle
Metformin
***
p < 0.0001
Position along apical-basolateral axis (μm) relative to the BBM
C
Area Under the Curve (Arbitrary Units)
****
Vehicle
Metformin
D
Control
Metformin
E
P-PKA substrate positive nuclei (%)
****
Vehicle
Metformin
F
GK Rat
Metformin / Vehicle
Glucose
Glucose
Glucose
Blood glucose (mg/dl)
OGTT
Time (hours)
G
GK Rat
Vehicle
Metformin daily
Metformin daily + single dose
Blood glucose (mg/dl)
OGTT
Time (min)
H
GK Rat
Vehicle
Metformin
Blood glucose (mg/dl)
IPGTT
Time (min)

Figure 2. Effects of a single dose of metformin (MET) in GK diabetic rats

(A–C) Effects of a single dose of MET (200 mg/kg) on SGLT1 abundance in the enterocyte BBM and (D–E) PKA activity in the jejunum. (A) Representative immunofluorescence images (n ≥ 18 per condition in total) of SGLT1 in the jejunum (SGLT1 in green; nuclei in blue, scale bar, 50 μm) and (B and C) corresponding quantification in 3–4 animals per group (6 technical replicates each) (AU: Arbitrary Unit).

(D and E) Representative immunofluorescence images (n > 6 in total) of phosphorylated PKA substrates (in green) in jejunum and (E) corresponding quantification in 3–4 animals per group. Nuclei appear in blue. ****, $p < 0.0001$ by Student's *t* test (C and E) and ***, $p < 0.001$ by two-way ANOVA and Sidak's test for multiple comparisons, position along the apical-basolateral axis x MET, MET vs. vehicle (B).

(F) Effects on blood glucose of a single dose of MET (200 mg/kg) given 1 h prior to the first OGTT and during the following 16 h with two additional OGTTs (1 g/kg) simulating different times of meal intake (*$p < 0.05$, two-way ANOVA and Sidak's test for multiple comparisons, MET vs. vehicle).

(G) Effects on blood glucose of a daily dose of vehicle (black line with closed dots) or MET (red line with open dots) (200 mg/kg every night, for 7 days) versus MET daily plus one additional dose (200 mg/kg) given by gavage 1 h prior to the oral glucose challenge (red line with closed dots). (*$p < 0.05$, two-way ANOVA and Sidak's test for multiple comparisons, MET daily plus one single dose vs. vehicle and MET daily).

(H) Effects on blood glucose of a single dose of oral MET on glycemia 1 h prior to the intraperitoneal glucose challenge (no significant difference in MET vs. vehicle, two-way ANOVA). All data are mean ± SEM.

the BBM and apical uptake of AMG are correlated in Caco-2/TC7 cells (data not shown). To assess the persistence in time of this acute effect of MET, we repeated this experiment in cells under washout conditions. SGLT1 abundance at the apical membrane returned to vehicle levels at 3 h compared to the 1 h time point and fully normalized after 9 h (Figure 1D). These changes in apical SGLT1 density were not accompanied by modifications in the overall mRNA expression of *SLC5A1* or other gluco-transporter genes in the enterocyte (Figure S1).

A single oral dose of MET reduces PGR *in vivo*

To confirm the physiological relevance of the transient effect of MET observed *in vitro*, we evaluated the changes in PGR in different animal models. First, Goto-Kakizaki (GK) diabetic rats were treated with a single oral dose of MET 200 mpk, which was based on the human-animal dose relationship and the principle of normalization to body surface area (i.e., allometric scaling).[32] One hour later, rats were either killed for immunohistological analysis or submitted to an oral glucose tolerance test (OGTT). Rats receiving MET displayed a lower apical density of SGLT1 in the jejunum compared to rats treated with vehicle (Figures 2A–2C) together with lower levels of phosphorylated PKA substrates in enterocytes (Figures 2D and 2E) and a lower PGR (Figure 2F). To evaluate the sustainability and reversibility of MET, rats received two extra glucose challenges at 6 h intervals. The marked lowering of PGR observed after the first glucose challenge (1 h after the MET dosing) compared to vehicle treatment was attenuated at 6 h and fully normalized at 12 h (Figure 2F). The effect of MET on PGR varied with the time interval between its administration and that of oral glucose and was maximal at 1 h (Figure S2A). Similarly, the PGR reduction by MET was dose-dependent, being maximal at 200 mg/kg, though effective even at a 50 mg/kg dose (Figure S2B). To distinguish the acute versus chronic effect of MET, GK rats received one single daily dose of MET (200 mpk) for one week. The PGR was unchanged when the oral glucose challenge was performed 12 h after the last MET dose in the daily group. In contrast, a single supplementary dose of MET, administered 1 h before the oral glucose load further reduced PGR in the same rats (Figure 2G). Moreover, after 1 h of MET administration, an intraperitoneal glucose tolerance test was performed without significant changes in glucose levels (Figure 2H); these results are in line with previous data in GK rats, which described a greater effect of MET at feeding[33] and also as measured by intravenous glucose tolerance test.[34] Together, these various acute effects of MET did not modify the expression of the main intestinal gluco-transporter genes in GK rats (Figure S2C).

The lower PGR after a single dose of MET requires SGLT1 expression but not GLUT2

We also confirmed the effect of a single dose of MET on PGR during an OGTT in C57BL/6 mice compared to vehicle-treated mice (Figure 3A). We then repeated these experiments in genetically modified mice[35] lacking SGLT1 or GLUT2; as in mammals, the active transport of dietary glucose from the intestinal lumen relies primarily on SGLT1 and, to a lesser extent, on GLUT2.[36] As expected, the PGR was diminished in untreated Sglt1-KO mice, compared to their wild-type littermates (Figure S3A), while the PGR was not modified in Glut2-KO mice compared to their wild-type littermates (Figure S3B). However, a single oral dose of MET given 1 h prior to an oral glucose challenge significantly decreased PGR in Glut2-KO mice (Figure 3B), but not in Sglt1-KO mice (Figure 3C), indicating that the MET-induced reduction in PGR is dependent on SGLT1 expression.

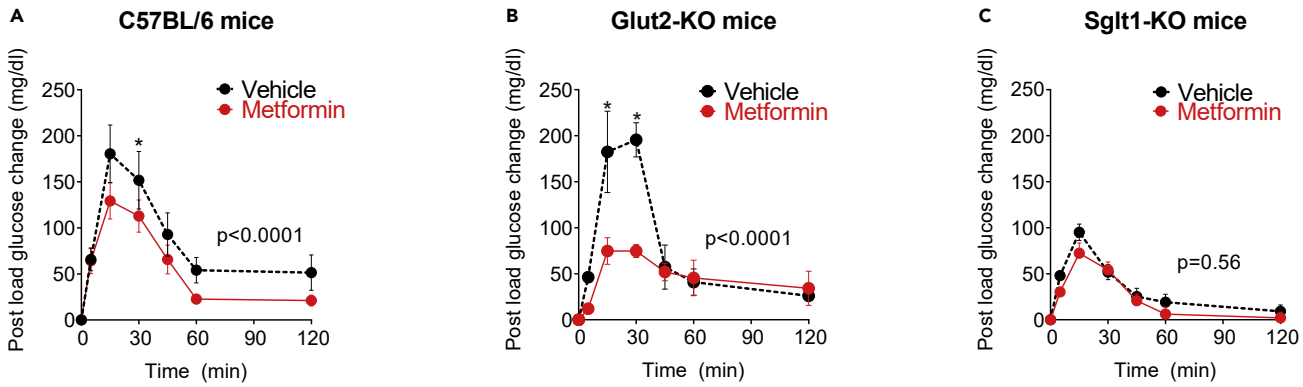

Figure 3. Effects of a single dose of metformin (MET) in wild-type or mutant mice

(A–C) Post-load glucose changes after a single dose of MET (200 mg/kg) given 1 h prior to an OGTT (glucose charge: 1 g/kg) (A) in normal C57BL/6 mice, (B) Glut2-KO mice, and (C) Sglt1 KO mice. (*$p < 0.05$, two-way ANOVA and Sidak's test for multiple comparisons, MET vs. vehicle, $n \geq 6$ per group). Data are mean ± SEM.

MET reduces intra-intestinal glucose absorption in mini-pigs

We next tested the effect of a single intraluminal dose of MET in mini-pigs. Each mini-pig was tested twice, after receiving a bolus of MET or vehicle via jejunostomy, followed 30 min later by a bolus of glucose and D-xylose, a non-metabolizable pentose routinely used in large animals and humans to estimate intestinal sugar absorption.[37,38] We found that MET decreased PGR (Figure 4A), as well as plasma insulin levels (Figure 4B), compared to vehicle-treated controls. We also found a diminished plasma appearance of luminal xylose (Figure 4C) in the MET-treated mini-pigs compared to the vehicle-treated controls. In addition, we saw an increase in GLP1 release in the MET group versus the vehicle-treated group (Figure 4D). Finally, a single dose of MET did not modify the expression of the main intestinal gluco-transporter genes in the mini-pigs (Figure S2D).

MET has distinct effects on systemic versus intraluminal ^{18}F-FDG transport

In clinical imaging with 2-(^{18}F)-fluoro-2-deoxy-D-glucose (^{18}F-FDG) PET-CT, chronic MET treatment is accompanied by a rise in the radiolabeling of the gut.[15,16,39] This phenomenon has been linked to an increased glucose uptake from the bloodstream into the enterocyte, which likely contributes to the glucose-lowering effects of MET[1,10,11,20] (Figure S5A). In GK rats, a single dose of MET tends to increase intestinal radioactivity after intravenous administration of ^{18}F-FDG as compared to vehicle-treated animals, an effect which is significant in rats treated with a daily MET dose (Figures 5A and 5B). However, this acute ^{18}F-FDG signal is not associated with a decrease in glycemia after the parenteral glucose challenge (Figure 2G).

Finally, we also used PET-CT dynamic imaging to objectify the intestinal passage of ^{18}F-FDG infused in the intestinal lumen, using a surgical-closed compartment system (Figures 5C and S5B). A single oral dose of MET administered 1 h prior to the luminal ^{18}F-FDG retained the radiotracer in the intestinal lumen (Figures 5D and 5E and Videos S1 and S2), reducing its appearance in the urinary bladder content (Figure 5F). This phenomenon explains the reduced PGR 1 h after a single dose of MET (Figure 2F). Similar results were obtained in healthy Wistar rats (Figure S4). Overall, these experiments provide direct evidence that MET treatment results in the retainment of carbohydrates in the intestinal lumen and interferes with intestinal glucose absorption.

DISCUSSION

The present study provides evidence of a primary gut effect of a single dose of MET on the intestinal absorption of ingested glucose and thus lowering of the PGR. We also showed that this effect of MET results from a transient decrease in the apical density and function of SGLT1 in the enterocyte. This gut-derived mechanism of action of MET is consistent with several recent clinical observations. In patients with T2D, a single dose of MET administered either orally[12] or directly in the jejunum[13] 1 h before a glucose challenge reduced PGR by 23% and 21%, respectively. A single oral dose of SGLT1 inhibitor administered prior to a meal also reduced PGR in healthy volunteers.[40] Moreover, the duodenal expression of SGLT1 protein is

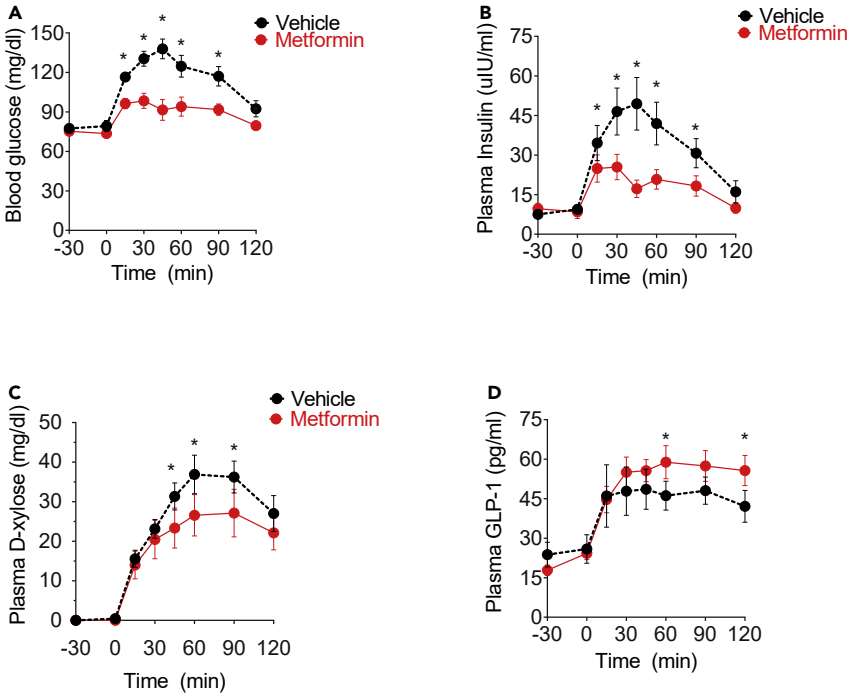

Figure 4. Effects of a single dose of metformin (MET) in mini-pigs

(A–D) Blood glucose, (B) plasma insulin, (C) plasma D-xylose, and (D) plasma GLP1 levels following a glucose + xylose bolus administered in mini-pigs (n = 10) through a jejunostomy, 30 min after a single oral dose of MET (25 mg/kg) or vehicle (*p < 0.05, two-way ANOVA and Sidak's test for multiple comparisons, MET vs. vehicle). Data are mean ± SEM.

increased in T2D and correlates with the PGR estimated by OGTT in subjects with various degrees of glucose tolerance.[41] Likewise, individuals carrying SGLT1 haplotypes associated with partial loss of function have lower 2-h blood glucose during an OGTT.[42] Mendelian randomization studies also estimated that SGLT1 loss of function reduces the overall incidence of T2D by 2% per year in these subjects.[42] This percentage is in line with the reduction in diabetes incidence observed in patients receiving chronic MET treatment in the Diabetes Prevention Program Outcomes Study (≈17% after 8 years).[43] Taken together with our findings here, the available clinical evidence supports the significant role played by the inhibition of SGLT1-mediated glucose intestinal absorption in the overall glucose-lowering effect of MET.

Here, we report that the transient decrease in SGLT1 density in the brush border of enterocytes following MET administration is accompanied by a decrease in PKA substrate phosphorylation in the rat jejunum. Although our study did not allow us to identify the molecular mechanism sustaining this direct effect of MET on the intestine, based on previous findings, we propose that the high amounts of MET that transiently accumulate in the intestine[9,30,44,45] change the intrinsic energy state of the enterocytes. At the molecular level, it has been demonstrated that high amounts of MET inhibit the electron transport chain of mitochondrial Complex I.[46,47] This inhibition was gradually alleviated depending on the dose and time of MET treatment, demonstrating the reversible nature of MET's mechanism of action.[48] The Complex I inhibition by MET decreases ATP production,[2] resulting in a concomitant increase in AMP levels that allosterically inhibit the cAMP–PKA pathway through suppression of adenylate cyclase.[49] We suggest that such a transient energy deficit occurs in enterocytes due to a rapid accumulation of the drug at the BBM, which is responsible for the transient reduction in the PKA-induced phosphorylation of SGLT1, a key event in the trafficking of this transporter to the apical membrane.[50] MET may indirectly inhibit SGLT1,[28] thus reducing sugar absorption by producing a temporary state of energy crisis in the enterocyte that interferes with the apical trafficking of this essential glucose transporter.

Alternative mechanisms of action for MET have been reported in the literature, including a recent report describing a metformin PEN2 axis in the intestine leading to AMPK activation independently of a change

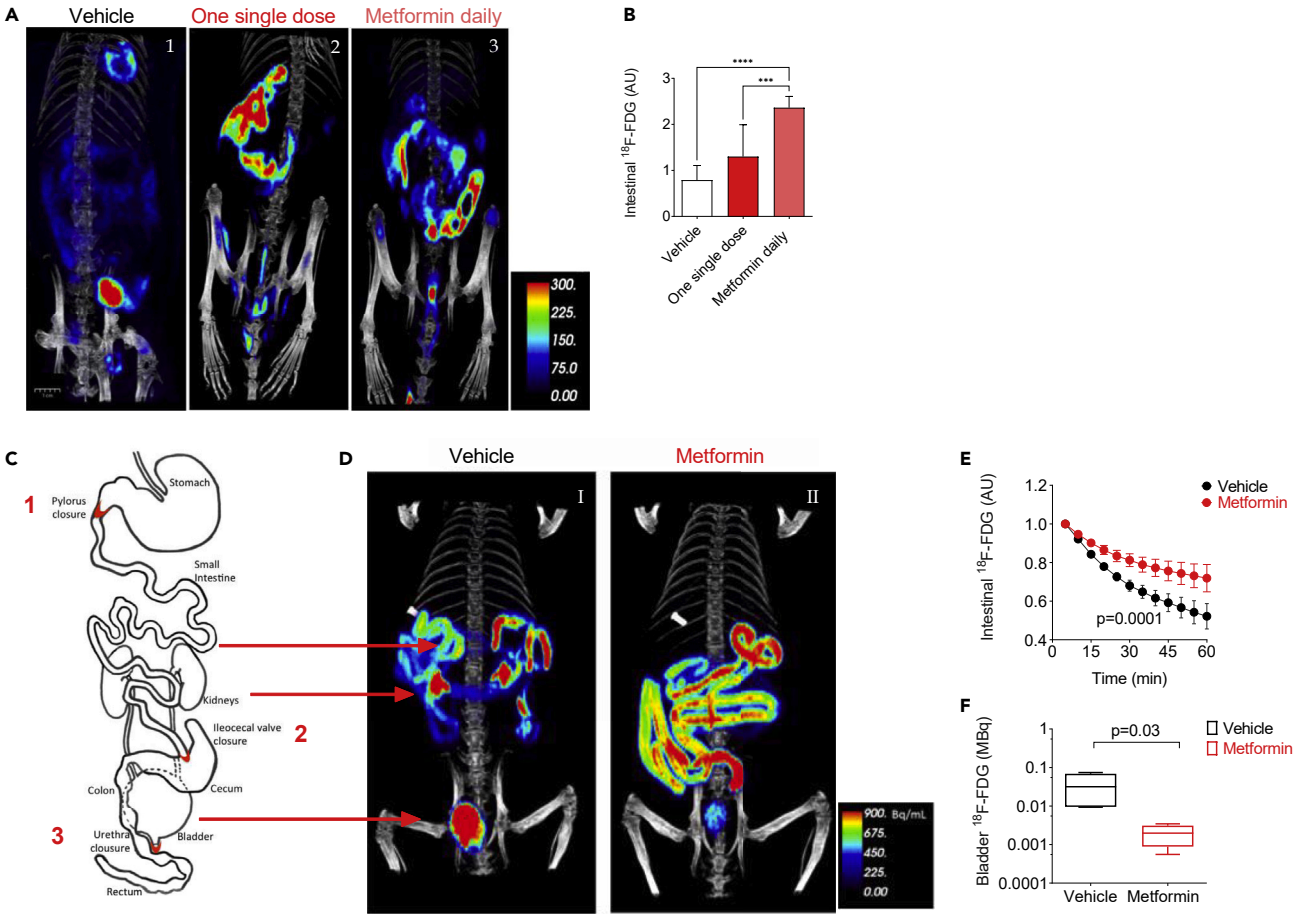

Figure 5. Effects of a single dose of metformin (MET) on intestinal ^{18}F-FDG absorption in GK rats

(A) Representative coronal, MIP-reconstructed slices of PET images of the abdominal area in GK rats after an intravenous administration of ^{18}F-FDG: [1] Vehicle/Control, [2] MET one single dose (1 h prior to the tracer administration), and [3] MET a daily dose (200 mg/kg every night, for 7 days). The ^{18}F-FDG signal was calculated by VOI analysis and normalized by the activity of the radiotracer in the femoral bone marrow.

(B) Quantification of ^{18}F-FDG signals in the intestine.

(C) Schematic diagram illustrating the closed compartments created by surgery to close the pylorus [1], ileocecal valve [2], and urethra [3].

(D) Representative coronal images from the PET-CT by MIP-reconstruction system of 12 frames after intestinal intraluminal administration of ^{18}F-FDG: [I] Vehicle/Control and [II] MET one single dose 1 h prior to ^{18}F-FDG oral administration.

(E) Time-activity curves (TACs) calculated by VOIs in the intestinal mass (ratio between the radioactivity in each frame divided by the value in the first frame) ($p = 0.0001$, two-way ANOVA, MET × time interaction, $n = 4$ per group).

(F) TACs of VOIs in the bladder content during the first 60 min of the study ($p = 0.03$, Mann-Whitney test, MET vs. Vehicle, $n = 4$ per group).

in the ratio of ATP to AMP.[51] Given these alternative mechanisms, the elucidation of the detailed molecular mechanism of action by which MET affects glucose absorption requires further exploration.

The effect of MET on intestinal sugar absorption demonstrated in the present study does not rule out the contribution of other intestinal or extra-intestinal mechanisms already proposed to explain the metabolic effects of this drug.[49] However, the reduction in the intestinal absorption of dietary glucose may also favor other gut-derived beneficial effects of MET. Likewise, by delaying the intestinal absorption of glucose, MET mechanically increases the amounts of glucose reaching the lower intestine, where it could contribute to increasing GLP-1 secretion,[21] to modulating the gut microbiota composition,[52] and to favoring the classical intestinal side effects associated with MET treatment.[53]

In conclusion, our findings further explain the gut-mediated clinical benefits of MET in the treatment of T2D.[9] The present results also challenge the current recommendations to administer this drug at bedtime

or after meals[54] and warrant a clinical evaluation of administration before meals to look for alternatives that enhance the gut-mediated effects of MET on glucose absorption. Finally, our study highlights the metabolic benefits induced by the modulation of SGLT1 activity in the gut.

Limitations of the study

Our study clearly shows that MET administered 1 h before a glucose challenge in different animal models reduces the systemic blood PGR. Since this effect is evident from the beginning of the OGTT time course, we believe that it is mainly due to an effect of MET on glucose absorption. Nevertheless, it is important to take into account that MET could impact many other factors. Regarding the concentration of 10 mM MET used in the culture media of intestinal epithelial cells, while it appears to be supraphysiological, this concentration was estimated to closely resemble the concentration of MET found in the alimentary chyme to which intestinal epithelial cells are apically exposed 1 h after the ingestion of a single dose of MET. Even so, it would be important to measure MET levels in jejunum tissue samples in response to an acute MET dose in animal models to confirm this choice. Finally, the effect of MET on AMPK activation in intestinal samples was not determined in this study. Thus, it would be important to set up follow-up studies to gain a greater mechanistic insight into the means by which MET sustains its direct effect on glucose transporter trafficking in enterocytes.

STAR★METHODS

Detailed methods are provided in the online version of this paper and include the following:

- KEY RESOURCES TABLE
- RESOURCE AVAILABILITY
  - Lead contact
  - Materials availability
  - Data and code availability
- EXPERIMENTAL MODEL AND SUBJECT DETAILS
  - Animals
  - Caco-2/TC7 cell line
- METHOD DETAILS
  - AMG uptake by Caco-2/TC7 cells
  - Immunohistology of Caco-2/TC7 cells
  - RNA extraction and RT-QPCR of Caco-2/TC7 cells
  - Western blot analysis of Caco-2/TC7 cells
  - Oral and intraperitoneal carbohydrates tolerance test in rodents
  - Immunohistological analysis in jejunum rat
  - Intrajejunal test in the mini-pig model for glucose tolerance and blood samples
  - RNA extraction and RT-QPCR on animal tissue
  - MicroPET test in rodents
- QUANTIFICATION AND STATISTICAL ANALYSIS

SUPPLEMENTAL INFORMATION

Supplemental information can be found online at https://doi.org/10.1016/j.isci.2023.106057.

ACKNOWLEDGMENTS

We thank Beatrice Duthoit and Hugo Bonvalet for their technical support on cell culture and molecular biology, and Meryem Tardivel and Antonino Bongiovanni of the BICeL-IFR114 Facility for access to systems and technical advice. Special thanks to the animal facility Dhure (University and Hospital Department for Experimental Research and Learning), especially Michel Pottier, Arnold Dive, Martin Fourdrinier, and Franck Stevendart. This work was supported by the Agence Nationale de la Recherche (ANR) grants "European Genomic Institute for Diabetes" EGID, ANR-10-LABX-0046, "Met-Intestin", ANR-18-CE14-0028, "MIGAD" ANR 21-CE45-0017 and the frame program Investissements d'Avenir I-SITE ULNE/ANR-16-IDEX-0004 ULNE, and the "Fondation Francophone de Recherche sur le Diabète (FFRD-2015-1).

AUTHOR CONTRIBUTIONS

L.Z. and F.P. conceived and performed experiments, wrote the manuscript, and analyzed the data. O.B., V.T., S.P., and S.L. performed *in vitro* experiments and analyzed the data. L.Z., T.H., J.T., C.M., and A.Q. oversaw animal welfare and performed *in vivo* experiments. H.K., M.M., D.Z., and B.T. provided the KO animals. L.Z., F.A., and D.H. performed the PET-CT imaging tests and analysis. C.B., V.G., M.D., V.R., J.K.C., N.D.D., L.B.B., B.D., M.C.V., B.S., and B.L. performed specific experiments, analyzed the data, edited the manuscript, and provided expertise and feedback. F.P. designed and supervised the whole project and edited the final version of manuscript and secured funding.

DECLARATION OF INTERESTS

The authors declare no competing interests.

Received: September 12, 2022
Revised: December 18, 2022
Accepted: January 20, 2023
Published: January 25, 2023

REFERENCES

1. Rena, G., Hardie, D.G., and Pearson, E.R. (2017). The mechanisms of action of metformin. Diabetologia *60*, 1577–1585. https://doi.org/10.1007/S00125-017-4342-Z.

2. Vancura, A., Bu, P., Bhagwat, M., Zeng, J., and Vancurova, I. (2018). Metformin as an anticancer agent. Trends Pharmacol. Sci. *39*, 867–878. https://doi.org/10.1016/j.tips.2018.07.006.

3. Hunter, R.W., Hughey, C.C., Lantier, L., Sundelin, E.I., Peggie, M., Zeqiraj, E., Sicheri, F., Jessen, N., Wasserman, D.H., and Sakamoto, K. (2018). Metformin reduces liver glucose production by inhibition of fructose-1-6-bisphosphatase. Nat. Med. *24*, 1395–1406. https://doi.org/10.1038/s41591-018-0159-7.

4. Madiraju, A.K., Qiu, Y., Perry, R.J., Rahimi, Y., Zhang, X.M., Zhang, D., Camporez, J.P.G., Cline, G.W., Butrico, G.M., Kemp, B.E., et al. (2018). Metformin inhibits gluconeogenesis via a redox-dependent mechanism in vivo. Nat. Med. *24*, 1384–1394. https://doi.org/10.1038/s41591-018-0125-4.

5. Jackson, R.A., Hawa, M.I., Jaspan, J.B., Sim, B.M., DiSilvio, L., Featherbe, D., and Kurtz, A.B. (1987). Mechanism of metformin action in non-insulin-dependent diabetes. Diabetes *36*, 632–640. https://doi.org/10.2337/diab.36.5.632.

6. Stumvoll, M., Nurjhan, N., Perriello, G., Dailey, G., and Gerich, J.E. (1995). Metabolic effects of metformin in non-insulin-dependent diabetes mellitus. N. Engl. J. Med. *333*, 550–554. https://doi.org/10.1056/nejm199508313330903.

7. Turban, S., Stretton, C., Drouin, O., Green, C.J., Watson, M.L., Gray, A., Ross, F., Lantier, L., Viollet, B., Hardie, D.G., et al. (2012). Defining the contribution of AMP-activated protein kinase (AMPK) and protein kinase C (PKC) in regulation of glucose uptake by metformin in skeletal muscle cells. J. Biol. Chem. *287*, 20088–20099. https://doi.org/10.1074/jbc.M111.330746.

8. Adak, T., Samadi, A., Ünal, A.Z., and Sabuncuoğlu, S. (2018). A reappraisal on metformin. Regul. Toxicol. Pharmacol. *92*, 324–332. https://doi.org/10.1016/J.YRTPH.2017.12.023.

9. Buse, J.B., DeFronzo, R.A., Rosenstock, J., Kim, T., Burns, C., Skare, S., Baron, A., and Fineman, M. (2016). The primary glucose-lowering effect of metformin resides in the gut, not the circulation: results from short-term pharmacokinetic and 12-week dose-ranging studies. Diabetes Care *39*, 198–205. https://doi.org/10.2337/dc15-0488.

10. McCreight, L.J., Bailey, C.J., and Pearson, E.R. (2016). Metformin and the gastrointestinal tract. Diabetologia *59*, 426–435. https://doi.org/10.1007/S00125-015-3844-9.

11. Wu, T., Horowitz, M., and Rayner, C.K. (2017). New insights into the anti-diabetic actions of metformin: from the liver to the gut. Expert Rev. Gastroenterol. Hepatol. *11*, 157–166. https://doi.org/10.1080/17474124.2017.1273769.

12. Walford, G.A., Colomo, N., Todd, J.N., Billings, L.K., Fernandez, M., Chamarthi, B., Warner, A.S., Davis, J., Littleton, K.R., Hernandez, A.M., et al. (2015). The study to understand the genetics of the acute response to metformin and glipizide in humans (SUGAR-MGH): design of a pharmacogenetic resource for type 2 diabetes. PLoS One *10*, e0121553. https://doi.org/10.1371/journal.pone.0121553.

13. Borg, M.J., Bound, M., Grivell, J., Sun, Z., Jones, K.L., Horowitz, M., Rayner, C.K., and Wu, T. (2019). Comparative effects of proximal and distal small intestinal administration of metformin on plasma glucose and glucagon-like peptide-1, and gastric emptying after oral glucose, in type 2 diabetes. Diabetes Obes. Metab. *21*, 640–647. https://doi.org/10.1111/dom.13567.

14. Sato, D., Morino, K., Nakagawa, F., Murata, K., Sekine, O., Beppu, F., Gotoh, N., Ugi, S., and Maegawa, H. (2017). Acute effect of metformin on postprandial hypertriglyceridemia through delayed gastric emptying. Int. J. Mol. Sci. *18*, 1282. https://doi.org/10.3390/ijms18061282.

15. Gontier, E., Fourme, E., Wartski, M., Blondet, C., Bonardel, G., le Stanc, E., Mantzarides, M., Foehrenbach, H., Pecking, A.P., and Alberini, J.L. (2008). High and typical 18F-FDG bowel uptake in patients treated with metformin. Eur. J. Nucl. Med. Mol. Imaging *35*, 95–99. https://doi.org/10.1007/S00259-007-0563-6.

16. Koffert, J.P., Mikkola, K., Virtanen, K.A., Andersson, A.M.D., Faxius, L., Hällsten, K., Heglind, M., Guiducci, L., Pham, T., Silvola, J.M.U., et al. (2017). Metformin treatment significantly enhances intestinal glucose uptake in patients with type 2 diabetes: results from a randomized clinical trial. Diabetes Res. Clin. Pract. *131*, 208–216. https://doi.org/10.1016/j.diabres.2017.07.015.

17. Yang, M., Darwish, T., Larraufie, P., Rimmington, D., Cimino, I., Goldspink, D.A., Jenkins, B., Koulman, A., Brighton, C.A., Ma, M., et al. (2021). Inhibition of mitochondrial function by metformin increases glucose uptake, glycolysis and GDF-15 release from intestinal cells. Sci. Rep. *11*, 2529. https://doi.org/10.1038/S41598-021-81349-7.

18. Brønden, A., Albér, A., Rohde, U., Gasbjerg, L.S., Rehfeld, J.F., Holst, J.J., Vilsbøll, T., and Knop, F.K. (2018). The bile acid-sequestering resin sevelamer eliminates the acute GLP-1 stimulatory effect of endogenously released bile acids in patients with type 2 diabetes. Diabetes Obes. Metab. *20*, 362–369. https://doi.org/10.1111/dom.13080.

19. Napolitano, A., Miller, S., Nicholls, A.W., Baker, D., van Horn, S., Thomas, E., Rajpal, D., Spivak, A., Brown, J.R., and Nunez, D.J. (2014). Novel gut-based pharmacology of metformin in patients with type 2 diabetes

mellitus. PLoS One *9*, e100778. https://doi.org/10.1371/journal.pone.0100778.

20. Sansome, D.J., Xie, C., Veedfald, S., Horowitz, M., Rayner, C.K., and Wu, T. (2020). Mechanism of glucose-lowering by metformin in type 2 diabetes: role of bile acids. Diabetes Obes. Metab. *22*, 141–148. https://doi.org/10.1111/DOM.13869.

21. Bahne, E., Sun, E.W.L., Young, R.L., Hansen, M., Sonne, D.P., Hansen, J.S., Rohde, U., Liou, A.P., Jackson, M.L., de Fontgalland, D., et al. (2018). Metformin-induced glucagon-like peptide-1 secretion contributes to the actions of metformin in type 2 diabetes. JCI Insight *3*, e93936. https://doi.org/10.1172/JCI.INSIGHT.93936.

22. Bauer, P.v., Duca, F.A., Waise, T.M.Z., Rasmussen, B.A., Abraham, M.A., Dranse, H.J., Puri, A., O'Brien, C.A., and Lam, T.K.T. (2018). Metformin alters upper small intestinal microbiota that impact a glucose-SGLT1-sensing glucoregulatory pathway. Cell Metab. *27*, 101–117.e5. https://doi.org/10.1016/j.cmet.2017.09.019.

23. Rodriguez, J., Hiel, S., and Delzenne, N.M. (2018). Metformin: old friend, new ways of action-implication of the gut microbiome? Curr. Opin. Clin. Nutr. Metab. Care *21*, 294–301. https://doi.org/10.1097/MCO.0000000000000468.

24. Ikeda, T., Iwata, K., and Murakami, H. (2000). Inhibitory effect of metformin on intestinal glucose absorption in the perfused rat intestine. Biochem. Pharmacol. *59*, 887–890. https://doi.org/10.1016/S0006-2952(99)00396-2.

25. Wilcock, C., and Bailey, C.J. (1991). Reconsideration of inhibitory effect of metformin on intestinal glucose absorption. J. Pharm. Pharmacol. *43*, 120–121. https://doi.org/10.1111/j.2042-7158.1991.tb06645.x.

26. Lenzen, S., Lortz, S., and Tiedge, M. (1996). Effects of metformin on SGLT1, GLUT2, and GLUT5 hexose transporter gene expression in small intestine from rats. Biochem. Pharmacol. *51*, 893–896. https://doi.org/10.1016/0006-2952(95)02243-0.

27. Sakar, Y., Meddah, B., Faouzi, M.Y.A., Cherrah, Y., Bado, A., and Ducroc, R. (2010). Metformin-induced regulation of the intestinal d-glucose transporters. J. Physiol. Pharmacol. *61*, 301–307.

28. Horakova, O., Kroupova, P., Bardova, K., Buresova, J., Janovska, P., Kopecky, J., and Rossmeisl, M. (2019). Metformin acutely lowers blood glucose levels by inhibition of intestinal glucose transport. Sci. Rep. *9*, 6156. https://doi.org/10.1038/s41598-019-42531-0.

29. Foretz, M., Guigas, B., and Viollet, B. (2019). Understanding the glucoregulatory mechanisms of metformin in type 2 diabetes mellitus. Nat. Rev. Endocrinol. *15*, 569–589. https://doi.org/10.1038/s41574-019-0242-2.

30. Bailey, C.J., Wilcock, C., and Scarpello, J.H.B. (2008). Metformin and the intestine. Diabetologia *51*, 1552–1553. https://doi.org/10.1007/s00125-008-1053-5.

31. Kimmich, G.A., and Randles, J. (1981). alpha-Methylglucoside satisfies only Na+-dependent transport system of intestinal epithelium. Am. J. Physiol. *241*, C227–C232. https://doi.org/10.1152/AJPCELL.1981.241.5.C227.

32. Reagan-Shaw, S., Nihal, M., and Ahmad, N. (2008). Dose translation from animal to human studies revisited. FASEB J *22*, 659–661. https://doi.org/10.1096/FJ.07-9574LSF.

33. Yoshida, T., Okuno, A., Tanaka, J., Takahashi, K., Nakashima, R., Kanda, S., Ogawa, J., Hagisawa, Y., and Fujiwara, T. (2009). Metformin primarily decreases plasma glucose not by gluconeogenesis suppression but by activating glucose utilization in a non-obese type 2 diabetes Goto-Kakizaki rats. Eur. J. Pharmacol. *623*, 141–147. https://doi.org/10.1016/j.ejphar.2009.09.003.

34. Franco, C.C.D.S., Miranda, R.A., De Oliveira, J.C., Barella, L.F., Agostinho, A.R., Prates, K.V., Malta, A., Trombini, A.B., Torrezan, R., Gravena, C., et al. (2014). Protective effect of metformin against walker 256 tumor growth is not dependent on metabolism improvement. Cell. Physiol. Biochem. *34*, 1920–1932. https://doi.org/10.1159/000366390.

35. Gorboulev, V., Schürmann, A., Vallon, V., Kipp, H., Jaschke, A., Klessen, D., Friedrich, A., Scherneck, S., Rieg, T., Cunard, R., et al. (2012). Na +-D-glucose cotransporter SGLT1 is pivotal for intestinal glucose absorption and glucose-dependent incretin secretion. Diabetes *61*, 187–196. https://doi.org/10.2337/db11-1029.

36. Sala-Rabanal, M., Ghezzi, C., Hirayama, B.A., Kepe, V., Liu, J., Barrio, J.R., and Wright, E.M. (2018). Intestinal absorption of glucose in mice as determined by positron emission tomography. J. Physiol. *596*, 2473–2489. https://doi.org/10.1113/JP275934.

37. Baud, G., Daoudi, M., Hubert, T., Raverdy, V., Pigeyre, M., Hervieux, E., Devienne, M., Ghunaim, M., Bonner, C., Quenon, A., et al. (2016). Bile diversion in roux-en-y gastric bypass modulates sodium-dependent glucose intestinal uptake. Cell Metab. *23*, 547–553. https://doi.org/10.1016/j.cmet.2016.01.018.

38. Craig, R.M., and Ehrenpreis, E.D. (1999). D-xylose testing. J. Clin. Gastroenterol. *29*, 143–150. https://doi.org/10.1097/00004836-199909000-00008.

39. Ito, J., Nogami, M., Morita, Y., Sakaguchi, K., Komada, H., Hirota, Y., Sugawara, K., Tamori, Y., Zeng, F., Murakami, T., and Ogawa, W. (2021). Dose-dependent accumulation of glucose in the intestinal wall and lumen induced by metformin as revealed by 18 F-labelled fluorodeoxyglucose positron emission tomography-MRI. Diabetes Obes. Metab. *23*, 692–699. https://doi.org/10.1111/DOM.14262.

40. Dobbins, R.L., Greenway, F.L., Chen, L., Liu, Y., Breed, S.L., Andrews, S.M., Wald, J.A., Walker, A., and Smith, C.D. (2015). Selective sodium-dependent glucose transporter 1 inhibitors block glucose absorption and impair glucose-dependent insulinotropic peptide release. Am. J. Physiol. Gastrointest. Liver Physiol. *308*, G946–G954. https://doi.org/10.1152/ajpgi.00286.

41. Fiorentino, T.V., Suraci, E., Arcidiacono, G.P., Cimellaro, A., Mignogna, C., Presta, I., Andreozzi, F., Hribal, M.L., Perticone, F., Donato, G., et al. (2017). Duodenal sodium/glucose cotransporter 1 expression under fasting conditions is associated with postload hyperglycemia. J. Clin. Endocrinol. Metab. *102*, 3979–3989. https://doi.org/10.1210/jc.2017-00348.

42. Seidelmann, S.B., Feofanova, E., Yu, B., Franceschini, N., Claggett, B., Kuokkanen, M., Puolijoki, H., Ebeling, T., Perola, M., Salomaa, V., et al. (2018). Genetic variants in SGLT1, glucose tolerance, and cardiometabolic risk. J. Am. Coll. Cardiol. *72*, 1763–1773. https://doi.org/10.1016/j.jacc.2018.07.061.

43. Diabetes Prevention Program Research Group (2019). Long-term effects of metformin on diabetes prevention: identification of subgroups that benefited most in the diabetes prevention program and diabetes prevention program outcomes study. Diabetes Care *42*, 601–608. https://doi.org/10.2337/DC18-1970.

44. Chung, H., Oh, J., Yoon, S.H., Yu, K.S., Cho, J.Y., and Chung, J.Y. (2018). A non-linear pharmacokinetic-pharmacodynamic relationship of metformin in healthy volunteers: an open-label, parallel group, randomized clinical study. PLoS One *13*, e0191258. https://doi.org/10.1371/JOURNAL.PONE.0191258.

45. Paleari, L., Burhenne, J., Weiss, J., Foersch, S., Roth, W., Parodi, A., Gnant, M., Bachleitner-Hofmann, T., Scherer, D., Ulrich, C.M., et al. (2018). High accumulation of metformin in colonic tissue of subjects with diabetes or the metabolic syndrome. Gastroenterology *154*, 1543–1545. https://doi.org/10.1053/J.GASTRO.2017.12.040.

46. El-Mir, M.Y., Nogueira, V., Fontaine, E., Avéret, N., Rigoulet, M., and Leverve, X. (2000). Dimethylbiguanide inhibits cell respiration via an indirect effect targeted on the respiratory chain complex I. J. Biol. Chem. *275*, 223–228. https://doi.org/10.1074/JBC.275.1.223.

47. Owen, M.R., Doran, E., and Halestrap, A.P. (2000). Evidence that metformin exerts its anti-diabetic effects through inhibition of complex 1 of the mitochondrial respiratory chain. Biochem. J. *348*, 607–614. https://doi.org/10.1042/0264-6021:3480607.

48. Bridges, H.R., Jones, A.J.Y., Pollak, M.N., and Hirst, J. (2014). Effects of metformin and other biguanides on oxidative phosphorylation in mitochondria. Biochem. J. *462*, 475–487. https://doi.org/10.1042/BJ20140620.

49. Wróbel, M.P., Marek, B., Kajdaniuk, D., Rokicka, D., Szymborska-Kajanek, A., and Strojek, K. (2017). Metformin - a new old drug. Endokrynol. Pol. *68*, 482–496. https://doi.org/10.5603/EP.2017.0050.

50. Subramanian, S., Glitz, P., Kipp, H., Kinne, R.K.H., and Castaneda, F. (2009). Protein kinase-a affects sorting and conformation of the sodium-dependent glucose co-transporter SGLT1. J. Cell. Biochem. *106*, 444–452. https://doi.org/10.1002/jcb.22025.

51. Ma, T., Tian, X., Zhang, B., Li, M., Wang, Y., Yang, C., Wu, J., Wei, X., Qu, Q., Yu, Y., et al. (2022). Low-dose metformin targets the lysosomal AMPK pathway through PEN2. Nature *603*, 159–165. https://doi.org/10.1038/S41586-022-04431-8.

52. Forslund, K., Hildebrand, F., Nielsen, T., Falony, G., Le Chatelier, E., Sunagawa, S., Prifti, E., Vieira-Silva, S., Gudmundsdottir, V., Pedersen, H.K., et al. (2015). Disentangling the effects of type 2 diabetes and metformin on the human gut microbiota Europe PMC Funders Group. Nature *528*, 262–266. https://doi.org/10.1038/nature15766.

53. Hammer, H.F., and Hammer, J. (2012). Diarrhea caused by carbohydrate malabsorption. Gastroenterol. Clin. North Am. *41*, 611–627. https://doi.org/10.1016/j.gtc.2012.06.003.

54. Bailey, C.J. (2017). Metformin: historical overview. Diabetologia *60*, 1566–1576. https://doi.org/10.1007/s00125-017-4318-z.

55. Tucker, G.T., Casey, C., Phillips, P.J., Connor, H., Ward, J.D., and Woods, H.F. (1981). Metformin kinetics in healthy subjects and in patients with diabetes mellitus. Br. J. Clin. Pharmacol. *12*, 235–246. https://doi.org/10.1111/J.1365-2125.1981.TB01206.X.

STAR★METHODS

KEY RESOURCES TABLE

REAGENT or RESOURCE	SOURCE	IDENTIFIER
Antibodies		
Rabbit Polyclonal anti-SGLT1 (1:100)	Millipore	Cat# 07-1417, RRID: AB_1587521
Rabbit Polyclonal anti-SGLT1 (1:250)	Abcam	Cat#Ab14686
Mouse Monoclonal anti-ZO1 (1:50)	Invitrogen	Cat# 33-9100, RRID: AB_2533147
Rabbit Polyclonal anti-AMPKα (1:1000)	Cell Signaling	Cat# 2532, RRID:AB_330331
Rabbit Monoclonal Anti-phospho-AMPKα (Thr172)	Cell Signaling	Cat# 2535, RRID: AB_331250
Mouse Monoclonal Anti-GAPDH (1:1000)	Santa Cruz	Cat# sc-32233, RRID:AB_627679
Mouse Polyclonal Anti-Hsp90α/β(1:1000)	BioLegend	at# 661802, RRID:AB_2564179
Goat Polyclonal HRP Anti-rabbit IgG (1:2000)	Sigma-Aldrich	Cat# A0545, RRID:AB_257896
Goat Polyclonal HRP Anti-mouse IgG (1:2000)	Millipore	Cat# AP124P, RRID:AB_90456
Chemicals, peptides, and recombinant proteins		
Metformin Sandoz® 1000 mg (*in vivo* experiments)	Sandoz – Novartis	3400936671010
Metformin (hydrochloride) (*in vitro* experiments)	MedChemExpress	HY-17471A/CS-1851
2-(^{18}F)-fluoro-2-deoxy-D-glucose (^{18}F-FDG)	CISBIO Internatinal	FDG-IBA-PA
D-Glucose	Sigma-Aldrich	G-8270
D-Xylose	Sigma-Aldrich	W-360600
α-Methyl-D-glucopyranoside (AMG)	Sigma-Aldrich	M9376
(14C)-α-Methyl-D-glucopyranoside (0.2 μCi/mL)	Perkin Elmer	NEC659050UC
Ketamine -Kétamine1000®	Virbac	03597132111010
Xylazine -Sedaxylan®	Dechra	08714225151530
Isoflorane - IsoFlo®	Zoetis	05414736033471
Critical commercial assays		
Free-Style\Optium – NeoH Glucometre	Abbot Diabetes Care Ltd	N°-71355-80
Colorimetric micro-method phloroglucinol Xylose	This paper	N/A
Insuline Ultrasensible Kit	Beckman Coulter	33410
GLP-1 RIA Kit	Millipore-IDS	GLP1T-36HK
Experimental models: Cell lines		
Caco-2/TC7	Lille University	N/A
Experimental models: Organisms/strains		
Rat: Goto-Kakizaki	Taconic M&B Company	GK/Mol Tac
Rat: Wistar	Janvier Labs	Ref. Albino rat Tyr^{c}/Tyr^{c}
Mouse: C57BL/6	Janvier Labs	Ref. C57BL/6Jrj
Mouse: *Sglt1* –/–	Wurzburg University	N/A
Mouse: *Glut2* –/–	Lausanne University	N/A
MiniPigs: Göttingen	Pannier's Breeding	N/A

(*Continued on next page*)

Continued

REAGENT or RESOURCE	SOURCE	IDENTIFIER
Oligonucleotides		
Primers for qPCR see Table S1.	This paper	N/A
Software and algorithms		
IRW 3.0 software	Siemens	Inveon RW 4.2
Graphpad Prism V.7	Graphpad	RRID:SCR_002798

RESOURCE AVAILABILITY

Lead contact

Further information and request for resources and reagents should be directed to and will be fulfilled by the Lead Contact, François Pattou (francois.pattou@univ-lille.fr), following an approval MTA between University of Lille and the receiving institution.

Materials availability

This study did not generate new unique reagents.

Data and code availability

- All data reported in this paper will be shared by the lead contact upon request.
- This paper does not report original code.
- Any additional information required to reanalyze the data reported in this paper is available from the lead contact upon request.

EXPERIMENTAL MODEL AND SUBJECT DETAILS

Animals

All animal procedures were performed in the Department of Experimental Research of Lille University (DHURE, Lille-Cedex, France) in accordance with French regulations for animal experiments and following European and French ethical rules. Rats and mice were housed under standard laboratory conditions (temperature 22°C +/− 2°C, humidity 35-60%) in a 12 h light/dark cycle and with tap water and regular food provided *ad libitum*.

Male Wistar and GK rats (12-24 week-old) weighing 300-400 g (Center Elevage Janvier (Le Genest-St-Isle, France) & Taconic M&B Company (Hudson, NY, USA)). Three different mouse strains were used: (1) C57BL/6 (Center Elevage Janvier (Le Genest-St-Isle, France) male wild type between 20 and 30 g (12-24 week-old), (2) whole-body Sglt1 knockout mice and their respective littermate (male – 12-24 week-old) were obtained from Department Tissue Engineering & Regenerative Medicine (TERM) University Hospital, Wurzburg, Germany, (3) Intestinal-specific Glut2 knockout mice and their respective littermate (male – 12-24 week-old) were obtained from Lausanne University, Lausanne, Switzerland. The Knockout animals received special food free of D-glucose and water *ad libitum*. A total of 10 healthy female young adult (1-3 years-old) Göttingen minipigs weighing 50 ± 8 kg (Pannier's Breeding) were housed in a temperature-controlled environment (21°C) with 12-h light/dark cycles and received regular food and water *ad libitum*.

Caco-2/TC7 cell line

Caco-2/TC7 cells were grown as previously described on Transwell systems. Cell culture reagents were obtained from Thermo Scientifics and micro-porous PET membrane inserts (23.1 mm, 3 μm pore size) from Corning. Caco-2/TC7 cells were routinely grown in plastic flasks under a humidified atmosphere containing 10% CO_2, at 37°C, in Dulbecco's modified essential medium containing 25 mM glucose and glutamax, supplemented with penicillin/streptomycin (100 IU/mL and 100 μg/mL, respectively), 1% non-essential amino acids, and 20% heat-inactivated fetal calf serum (FCS). To establish the intestinal barrier model for the assay, Caco-2/TC7 cells (between passages 40 and 55) were plated at a density of 0.25 × 10^6 cells per 6-well plate insert and grown in complete medium. Confluence was routinely reached 8 days after

seeding. Cells were then cultured in asymmetric conditions, with medium containing FCS in the lower compartment and serum-free medium in the upper compartment. Media were changed every day for three weeks.

METHOD DETAILS

AMG uptake by Caco-2/TC7 cells

Differentiated Caco-2/TC7 cells grown on Transwells were pre-incubated for 1 h in DMEM without glucose then 1 h in DMEM without glucose supplemented with 1% BSA free fatty acids (Sigma-Aldrich) in presence or absence of 10 mM MET (MedChemExpress). Specific experiments were set up to differentiate the acute effect of the administration of a single versus multiple doses of MET, to highlight the duration and the reversibility of MET's effects, and to assess possible desensitization. Uptake experiments were initiated by replacing the medium with medium containing 2 mM α-Methyl-D-glucopyranoside (AMG) (Sigma, M9376-100G) and [^{14}C]- α-Methyl-D-glucopyranoside (Perkin Elmer, NEC659050UC 0.2 μCi/mL). After incubation, the reaction was stopped by adding cold PBS containing phloretin 0.5 mM. Cells were washed 3 times with PBS and solubilized by adding 1 mL Solvable (PerkinElmer). The samples were analyzed in the scintillation counter TopCount (PerkinElmer). The concentration of metformin used *in vitro* was chosen to be roughly equivalent to the concentration in human intestinal lumen following oral administration as measured in Tucker et al.[55] and Bailey et al.[30]

Immunohistology of Caco-2/TC7 cells

At the end of a 1 hr-incubation in DMEM without glucose and 1 hr-treatment in presence or absence of 10 mM MET, cells were washed twice with PBS and fixed for 30 min with 4% paraformaldehyde (w/v) in PBS, then incubated for 1 h with 100 mmol/L L-Lysine and permeabilized by incubation during 5 min with TN buffer (Tris 20 mmol/L, pH 7.4, NaCl 0.5 mol/L) containing 0.1% Triton X-100, then extensively washed with TN buffer. Transwells were gently cut into 6 to 8 pieces then blocked using Image iT fix reagent (Life technologies) and overnight incubated at 4°C with the indicated primary antibodies. After extensive washing in TN buffer, Alexa-conjugated secondary antibodies (Molecular probe, 1:400) were incubated for 1 h. Cells were finally mounted using a mounting medium (Dako) containing Hoechst 33,342 (Sigma-Aldrich) at 1 mg/mL then examined using a LSM710 confocal microscope (Zeiss) in a sequential mode of acquisition. Anti-SGLT1 antibody (Millipore Cat# 07-1417, RRID: AB-1587521); anti-ZO-1 (Creative Diagnostics Cat# DCABH-3988, RRID: AB-2477799) were used in this analysis.

RNA extraction and RT-QPCR of Caco-2/TC7 cells

Total RNA from Caco-2/TC7 was isolated using Trizol reagent (Invitrogen, ThermoFisher). RNA quantity and purity were measured by Nanodrop device (ThermoScientific, ThermoFisher). Reverse transcription was performed using high capacity reverse transcription (Applied Biosystems). qPCR were performed using the Brillant II ultra-fast Sybr green qPCR Master mix (Agilent) with specific primers (Eurogentec) (Table S1) on an Mx3005 device (Agilent). mRNA levels of target genes were subsequently normalized to human TBP.

Western blot analysis of Caco-2/TC7 cells

Caco-2/TC7 cells were washed twice in PBS and harvested in lysis buffer containing 1% Nonidet P-40, 0.5% sodium deoxycholate, 0.1% SDS, protease inhibitor cocktail (Complete, Roche) and phosphatase inhibitor cocktail 3 (Sigma-Aldrich) in PBS. Samples were sonicated for 5 min (Bioruptor, Diagenode). Homogenates were centrifuged (16,000 x *g* – 10min–4°C) and supernatants stored at −20°C. Protein concentration was determined using the BCA protein assay (Pierce, ThermoFisher). Thirty to 40 μg of proteins were separated on a BOLT 4-12% Bis-Tris Plus gels (Invitrogen, ThermoFisher) then transferred to a nitrocellulose membrane. Membranes were blocked for 1 h with 5% BSA in Tris-buffered saline 0.1% tween. The membrane was then incubated overnight with primary antibodies (rabbit polyclonal anti-AMPKα, Cell Signaling, Cat# 2532, RRID: AB_330331; rabbit monoclonal anti-phospho-AMPKα (Thr172), Cell Signaling, Cat# 2535, RRID: AB_331250; mouse monoclonal Anti-GAPDH, Santa Cruz, Cat# sc-32233, RRID: AB_627679; and mouse polyclonal Anti-Hsp90α/β, Biolegend, Cat# 661802, RRID: AB_2564179) and after a 1 h-incubation period with horseradish peroxidase-conjugated secondary antibodies (Goat Polyclonal HRP Anti-rabbit IgG, Sigma-Aldrich, Cat# A0545, RRID: AB_257896; and Goat Polyclonal HRP Anti-mouse IgG, Millipore, Cat# AP124P, RRID: AB_90456) were used. Protein revelation was performed using the Super-Signal West

Dura Substrate (ThermoScientific, ThermoFisher) by chemiluminescence (Camera Gbox, SynGene) and band intensity was measured (Image Studio Lite, LI-COR Biosciences).

Oral and intraperitoneal carbohydrates tolerance test in rodents

Oral glucose tolerance test (OGTT) and intraperitoneal glucose tolerance test (IPGTT) were performed on conscious rats, following 18 h of fasting. Blood samples from fasted animals were first taken from the tail vein. MET was diluted in distilled water and given orally (200 mg/kg) 1 h before the load of glucose. The dose chosen was based onto the human-animal dose relationship and the principle of normalization to body surface area (ie, allometric scaling).[32] It was in agreement with Foretz et al.[29] Controls were given only distilled water as vehicle. Rats in the Wistar group were fed a 50% glucose fixed at 4 g/kg body weight and the GK rats group were fed a 50% glucose solution fixed at 1 g/kg body weight (according to the differences of a physiological versus a diabetic model). The mice (all strains) experiments for OGTT were similar with only 6 h of starvation and glucose 50% on 2 g/kg. All blood samples were taken by tail bleeds at 0, 15, 30, 60 and 120 min after glucose administration. Glucose determination in blood was run immediately using a Free-Style\Optium – NeoH Glucometre (Abbott, UK).

Immunohistological analysis in jejunum rat

GK rats were sacrificed 1 h after an oral challenge with metformin or vehicle and jejunum harvested. Immuno-fluorescent staining of SGLT1 (ab14686) in PFA-fixed and OCT embedded jejunum slices. Nuclei were counterstained with DAPI. Photos were obtained using a Leica DMI6000B microscope with 40x magnification. Fluorescent labeling for SGLT1 were quantified using ImageJ (plot profile tool) along an apical to basolateral axis crossing one enterocyte.

Intrajejunal test in the mini-pig model for glucose tolerance and blood samples

Mini-pigs were fasted overnight and premedicated with an intramuscular injection of ketamine (Ketamine1000, Virbac, France, 10 mg/kg of body weight) and xylazine (Sédaxylanc, Dechra Santé Animale, France, 2.5 mg/kg of body weight) prior to all surgical procedures. All surgical procedures were performed under general anesthesia, with a 4% concentration of isoflurane (IsoFlo, Zoetis, France) A single-lumen radiopaque silicone catheter (Hickman; Bard, Trappes, France) was initially placed in the jugular vein and exteriorized on the neck of the animal for repeated non-invasive blood samples. In the same intervention, we performed a middle laparotomy, measured 150 cm of jejunum from the Treitz angle and performed a posterior-lateral jejunostomy. After a few days of recovery, the glucose challenge was administered through the jejunostomy, with a solution containing D-glucose (25 mg/kg) + D-Xylose (30 g) + distilled water (30 mL). D-Xylose, a non-metabolized carbohydrate, is routinely used to estimate intestinal carbohydrate absorption. Glycemia was evaluated using a Free-Style\Optium – NeoH Glucometre (Abbott, UK). Blood venous samples were taken at −30, 0, 5, 15, 30, 45, 60, 90 and 120 min and immediately kept on ice until centrifugation at 5,000 rpm for 10 min. Plasma aliquots were stored at −80°C until analysis. D-xylose was measured by a colorimetric micro-method with phloroglucinol as previously described.[37] Commercially available radioimmunoassay kits were used for measurement of insulin (Beckman Coulter #33410, France), and total GLP-1 total kit RIA (GLP-1T-36HK, Millipore-IDS, France).

RNA extraction and RT-QPCR on animal tissue

Total RNA from different animal models was isolated using the Rneasy mini kit (Qiagen Inc., Courtaboeuf, France). RNA was cleaned using the Rnase-Free DnaseSet (Qiagen Inc., Courtaboeuf, France), and the RNA Integrity Number was checked using RNA StdSens Analysis kit (Biorad, Marnes-la-Coquette, France). For reverse-transcription, 1 μg RNA from each sample was converted to cDNA using the iScript cDNA synthesis kit (Biorad, Marnes-la-Coquette, France). Real-time PCR was performed with the SsoAdvanced Universal SYBR Green supermix (Biorad, Marnes-la-Coquette) using the CFX Connect Real-time System (Biorad, Marnes-la-Coquette, France). The following conditions were performed: 3 min denaturation at 95°C, followed by 40 cycles of 10 s at 95°C and 30 s at 60°C. Melting curves were performed for each reaction. Ct Values were normalized with RPL27 (Ribosomal Protein L27) housekeeping gene (see Table S1).

MicroPET test in rodents

A microPET-CT machine Inveon (Siemens Medical Solutions, Knoxville, TN, USA) was used for PET data acquisition. PET-CT scan acquisition with administration on ^{18}F-FDG was performed to study FDG kinetic on luminal and basolateral sides of the gut. One-single dose of MET was given orally (200 mg/kg) 1 h before

the load of ^{18}F-FDG. Controls were given only distilled water as vehicle. To avoid the possible confounding effect of gastric emptying, gut peristalsis and bladder voiding the ^{18}F-FDG was injected in the duodenum under general anesthesia and watertight compartments between the intestine, circulatory and urinary system were created by occluding pylorus, ileo-cecal valve and urethra.

To evaluate the luminal side dynamic intraduodenal direct administration of ^{18}F-FDG (8-10MBq) was done. Dynamic microPET studies were performed, rats with an intestinal catheter were anesthetized, and placed on the PET-CT holder, and after ^{18}F-FDG intraduodenal injection PET scan was initiated. To evaluate the basolateral side, intravenously administration of ^{18}F-FDG (35-40 MBq) via the tail vein was done. After 45 min after radiotracer injection rats were anesthetized in an induction box by inhalation of 2% isoflurane ant then positioned on microPET small animal holder, which allows for continuous anesthesia then the PET scan was initiated. After completion of the PET data acquisition, 15 min CT scans were performed to provide anatomical information and attenuation tissues coefficients. The PET acquired data were binned into 12 image frames of 5 min and were reconstructed using 3D OSEM/SP-MAP (Ordered Subset Expectation Maximization/Shifted Poisson Maximum *A Priori*) method with an attenuation correction. Using Inveon Research Workplace software (Preclinical Solutions, Siemens Medical Solutions USA, Inc., Knoxville, TN, USA), 3-dimensional regions of interest (VOIs) were manually drawn over the images. Assessment of ^{18}F-FDG intestinal kinetic was estimated by determining radiotracer concentration (MBq/mL) in intestinal compartment as a function of time. In each experiment, VOI kidneys, bladder, cecum and intestine were drawn and the activity of tracer in each VOI at 60 min was estimated using IRW 3.0 software. ^{18}F-FDG intestinal kinetic was obtained from the difference between the initial and final activities in the kidneys, bladder, and cecum VOIs. However, for the TEP images post-treatment for the evaluation of the basolateral side VOIs of the intestine, cecum, kidney, bladder and femoral bone marrow were drawn manually and corresponding TACs. For each organ, setting up a dedicated radioactivity threshold then delineated VOIs to all frames. Finally, the activity was normalized according to the activity of the femoral bone marrow.

QUANTIFICATION AND STATISTICAL ANALYSIS

The animals (mice, rats and pigs) were randomly divided assigned in the different groups (control vs metformin: oral/intraperitoneal or acute/chronic). The serum and histological samples were extracted by different investigators under the same protocol. No blinding during the application of experimental treatment (e.g., gavage of a test drug) but regular blinding during the data collection and analysis. No special exclusion criteria were applied beyond the parameters of the NC3R ARRIVE guidelines. A minimum of 6 samples was required in each group. Results are expressed as means $\pm$ SEM and were analyzed using 1-way or two-way ANOVA and U-Mann-Whitney where appropriate using GraphPad Prism 7.0 software (Graphpad software Inc., San Diego, CA). Differences were considered significant at $p < 0.05$. Power calculations were not performed, but the sample size for each group was chosen based on study feasibility and prior knowledge of statistical power from previously published experiments.